



EFFECT OF NANO- AND MICRO-PARTICLES ON FRACTURE CHARACTERISTIC OF HA/PLLA COMPOSITES

Tetsuo Takayama*, Mitsugu Todo**, Yasuharu Takenoshita*** and Akira Myoui****

*Graduate School, Kyushu University,

**Research Institute for Applied Mechanics, Kyushu University

***Faculty of Dental Science, Kyushu University

****Faculty of Medicine, Osaka University

Keywords: Poly(L-lactide), Hydroxyapatite, Biomaterial, Fracture toughness

Abstract

Effects of bimodal distribution of micro- and nano-HA particles on the mechanical properties such as bending strength, modulus and J-integral at crack initiation, J_{in} , of HA/PLLA composites were investigated. The Bending properties were improved by bimodal distribution. It is considered that in bimodal HA/PLLA, PLLA molecular chains are constrained by existence of HA particles, resulting in the reduction of deformation of molecular chains.

J_{in} was also effectively improved by bimodal distribution. Additional increase of dissipated energy due to dense ductile deformation of the matrix and debonding of the particle/matrix interfaces is thought to be the primary mechanism for the improvement of J_{in} .

1 Introduction

Bioabsorbable thermoplastics poly(L-lactic acid) (PLLA) has widely been used as a biomaterial for bone fixation devices in orthopedic and oral surgeries[1-2]. Recently, hydroxyapatite (HA) particles filled PLLA composites have been developed to improve the modulus, bioactivity and degradation rate of the PLLA implants. Many researchers have investigated the mechanical properties of such HA/PLLA composites; these results show that the mechanical properties of PLLA degraded due to dispersing HA particles [3-15]. Todo et al. investigated the relationship between the microstructure and the fracture behavior of four different kinds of HA/PLLA composites with four different sizes and shapes of the HA particles [16].

They found that the mode I critical energy release rate, G_{IC} , is maximized by micro-size HA particles, and that of HA/PLLA with nano-size particles is the lowest. They also found that G_{IC} of the composites are much lower than that of neat PLLA.

In the present study, HA/PLLA composites with micro-, nano- and micro/nano-HA particles were fabricated, and their mechanical properties such as bending and fracture properties were evaluated to assess the effect of bimodal particle distribution on those properties. Fracture mechanism was also characterized using a field-emission scanning electron microscope (FE-SEM). The macroscopic fracture property was then correlated with the microscopic deformation mechanism.

2 Experimental

2.1 Materials

Two kinds of HA particles (Sangi Co. Ltd) with different sizes were used as filler. They are called as micro (5 μ m) and nano (100nm), where the number in parentheses is the representative size. PLLA was used as matrix. HA/PLLA mixtures were prepared from PLLA pellets and HA particles using a conventional melt-mixer by mixing for 20min at a rotor speed of 50rpm at 190°C. The weight fraction of the HA particles was fixed at 10wt%, and for the composites having both micro and nano, the weight fraction was 5wt% for both the particles. The three kinds of HA/PLLA composites fabricated are denoted as μ -10, n-10 and μ -5/n-5, thereafter.

Plates of 140x140x2 mm³ were fabricated from those mixtures by re-melting at 190°C and pressed at 30MPa for 30min using a hot press. The plates were

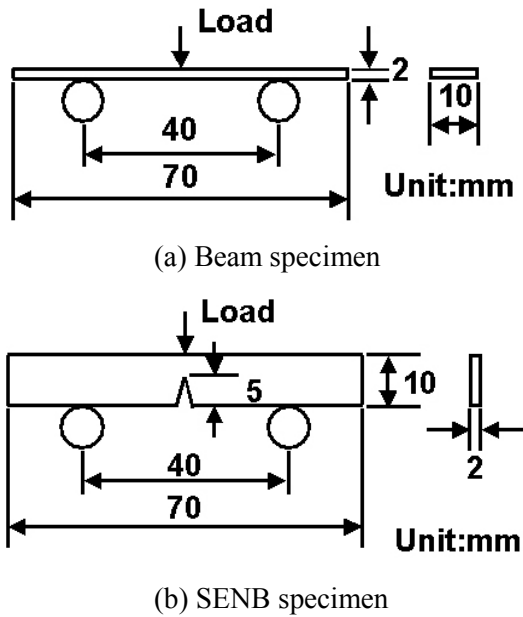


Fig.1 Geometries of specimen

then quenched to room temperature using a water-cooling system. Beam specimens and single edge notch bending (SENB) specimens were made from the HA/PLLA plates for bending and mode I fracture testing, respectively. The specimen geometries are shown in Fig.1

2.2 Bending testing

Three-point bending tests of the beam specimen (Fig.1(a)) were performed at a loading-rate of 10mm/min using a servohydraulic testing machine system. From these bending tests, bending modulus, E , and bending strength, σ_f , were calculated from the linear portion of load-displacement curves and maximum load, respectively, using the following formulae:

$$E = \frac{L^3}{4bh^3} S \text{ and } \sigma_f = \frac{3PL}{2bh^2} \quad (1)$$

where S is the initial slope of the load-displacement curve. L is the span, b and h are the width and thickness, respectively, and P is the maximum load.

2.3 Mode I fracture testing

Mode I fracture tests of the SENB specimens were performed at a loading-rate of 1 mm/min by a servohydraulic testing machine. The mode I critical J-integral at crack initiation, J_{in} , were evaluated using the following formula:

$$J_{in} = \frac{\eta U_{in}}{W(B-a)} \quad (2)$$

where U_{in} is the energy corresponding to the crack initiation defined as a point at which the rigidity of specimen decreased rapidly. B and W are the thickness and width of the SENB specimen, respectively, and a the initial crack length.

Fracture surfaces of the SENB specimens tested were also examined by FE-SEM to characterize the fracture mechanisms of the composites.

3 Results and Discussion

3.1 Bending properties

Typical load-displacement curves obtained from the bending tests are shown in Fig.2(a). The maximum load of μ -5/n-5 is the highest of all the three composites. n-10 exhibited the lowest peak load, suggesting dramatic decrease of bending strength. It is noted that sudden drop of load after the peak indicated brittle fracture of the composites. Results of E and σ_f measurements are shown in Fig.2(b) and (c), respectively. μ -5/n-5 exhibited the highest σ_f value. μ -10 was next to μ -5/n-5, and the difference between them was small. n-10 was the lowest and much lower than those of μ -10 and μ -5/n-5. μ -5/n-5 showed the highest value of E . E of n-10 was similar to that of μ -10. This result indicates that bimodal distribution of HA particles is more effective than monomodal distribution for increase of E of neat PLLA (E of neat PLLA is about 4 GPa).

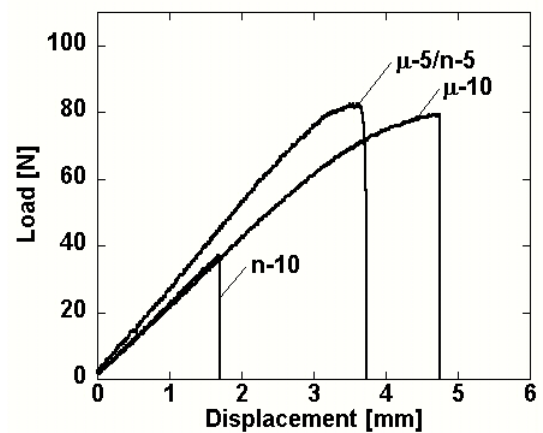
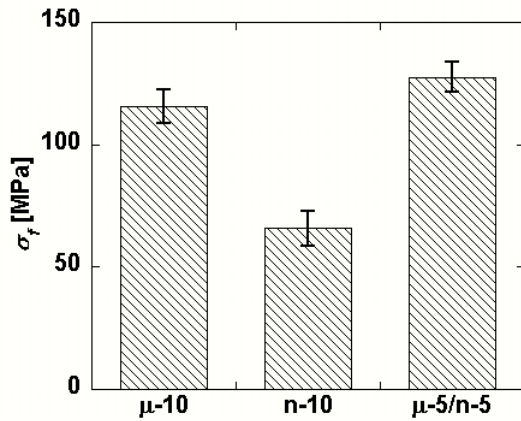
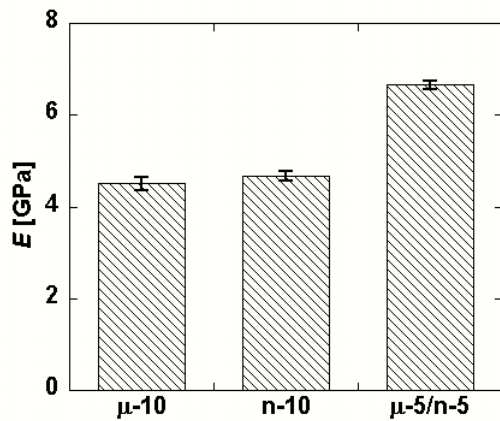


Fig.2 Load-displacement curves obtained from bending tests



(a) Bending strength



(b) Bending modulus

Fig.3 Bending mechanical properties

3.2 Mode I fracture property

Typical load-displacement curves obtained from the mode I fracture tests are shown in Fig.4. The maximum load of μ -5/n-5 is the highest of all the three composites, and n-10 showed the lowest, similar to the bending test results. J_{in} values of the composites are shown in Fig.5. μ -5/n-5 exhibited the highest value. J_{in} of n-10 is the lowest and much lower than that of μ -10 and μ -5/n-5.

It was found from the results of the mechanical tests that in terms of bending and mode I fracture properties, μ -5/n-5 exhibited the best performance, and n-10 possessed the lowest values. This result suggests that bimodal distribution of micro- and nano-HA particles is the most effective on these mechanical properties, and the nano-particles worked very effectively only under bimodal distribution condition.

3.3 Fracture mechanism

FE-SEM micrographs of the mode I fracture surfaces are shown in Fig.6. The direction of crack growth was from left to right. n-10 showed very smooth and flat surface (Fig.6(a)), indicating very low dissipated energy and therefore, corresponding to the lowest J_{in} value as shown in Fig.5. It is seen from Fig.6(b) that μ -10 showed rougher surface than n-10. It is noted that interfacial failure was observed at the interfaces between HA particles and PLLA matrix, and localized ductile deformation of the matrix was generated in the surroundings of the debonded particles. μ -5/n-5 showed a rough surface with interfacial failure at the HA/PLLA interfaces and localized plastic deformation in the surroundings of the particles, very similar to μ -10. However, in the crack-tip region (the left hand side of Fig.6(c)), dense ductile deformation of the matrix was formed, suggesting greater energy dissipation than μ -10 in which such crack-tip deformation was not generated.

It is thus presumed from these experimental results that in μ -5/n-5, the micro- and the nano-HA particles tended to be well distributed, and furthermore, by comparing Figs.6(b) and (c), it can be said that the micro-particles seemed to become smaller due to mechanical interaction between the micro- and the nano-particles during mixing process. In μ -5/n-5, the nano-particles were thought to be well distributed in the spaces between the PLLA molecular bundles as a result of such mechanical interaction. On the other hand, in monomodal distribution, the nano-particles tended to agglomerate during mixing process as seen in Fig.6(a), and these agglomerations are known to be easily fractured because of weak cohesion between the particles, resulting in low fracture energy. On the other hand, in μ -10, interfacial failures took place at the interfaces due to stress concentration in the surroundings of the micro-particles and localized plastic deformation was generated, resulting in more dissipated energy than in n-10. It is easily imagined that the cohesion force in the micro-particles is much greater than the aggregated nano-particles, therefore, interfacial failure preceded fracture of the micro-particles in μ -10.

4. Conclusions

In this study, effects of the bimodal distribution of HA particles on the mechanical properties such as bending strength, modulus and J-

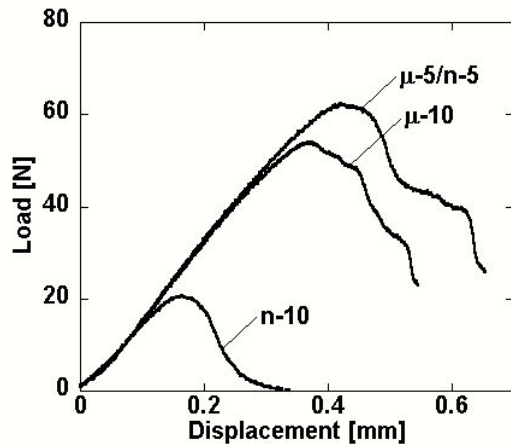


Fig.4 Load-displacement curves obtained from mode I fracture tests

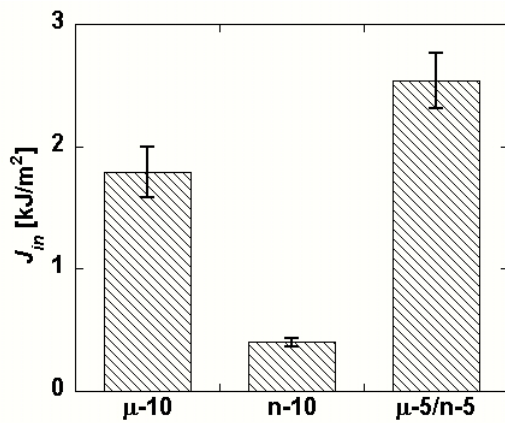
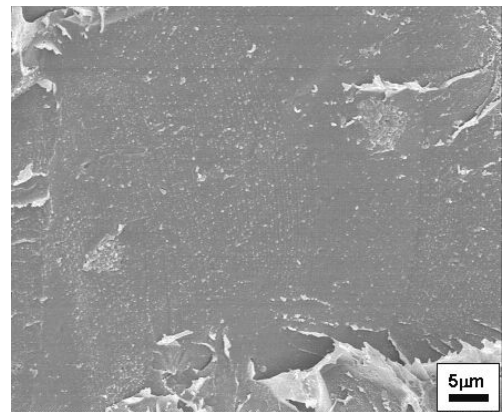


Fig.5 Critical J-integral at crack initiation

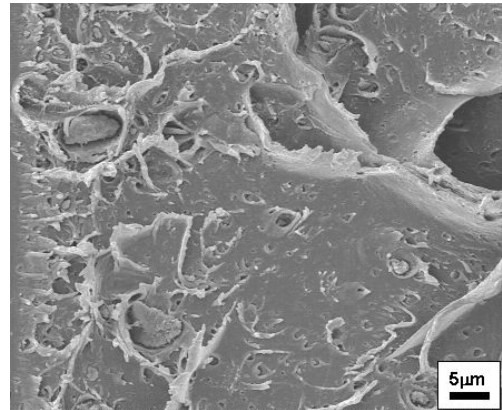
integral at crack initiation of HA/PLLA composites were investigated, and the following results were obtained:

(1) Bending properties of bimodal HA/PLLA exhibited the highest. It is considered that the nano-HA particles were gone into the gaps between molecular bundles, resulting in constraint of molecules. Mechanical interaction between the micro- and the nano-particles tended to reduce the size of the micro-particles, resulting in reduction of stress concentration.

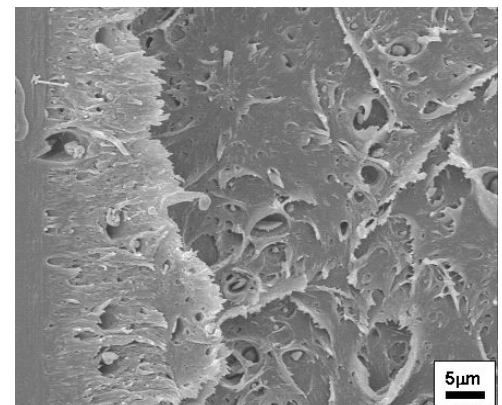
(2) J-integral at crack initiation of bimodal HA/PLLA also exhibited the highest. This reason is thought to be that dense ductile deformation of the matrix was generated in the crack-tip region, indicating higher energy dissipation than the other composites with monomodal distribution.



(a) n-10



(b) μ -10



(c) μ -5/n-5

Fig.6 FE-SEM micrographs of fracture surfaces.

References

- [1] Leenslag JW, Pennings AJ, Bos RRM, Rozema FR, Boering J. "Resorbable materials of poly(L-lactide). VI. Plates and screws for internal fracture fixation." *Biomaterials*, Vol.8, pp.70-73, 1987.
- [2] Bostman OM. "Absorbable implants for the fixation of fractures." *J Bone Joint Surgery*, Vol.73-A, No.1, pp.148-153, 1991.
- [3] Shikinami Y, Okuno M, "Bioresorbable devices made of forged composites of hydroxyapatite(HA) particles and poly-L-lactide(PLLA): Part.I Basic characteristics" *Biomaterials*, Vol.20, pp.859-877, 1999.
- [4] Yasunaga T, Matsusue Y, Furukawa T, Shikinami Y, Okuno M, Nakamura T, "Bonding behavior of ultrahigh strength unsintered hydroxyapatite particles/poly(L-lactide) composites to surface of tibial cortex in rabbits" *J Biomed Mater Res*, Vol.47, pp.412-419, 1999.
- [5] Kasuga T, Ota Y, Nogami M, Abe Y, "Preparation and mechanical properties of poly(lactic acid) containing hydroxyapatite fibers" *Biomaterials*, Vol.22, No.1, pp.19-23, 2001.
- [6] Rizzi SC, Heath DJ, Coombes AGA, Bock N, Textor M, Downes S, "Biodegradable polymer/hydroxyapatite composites: Surface analysis and initial attachment of human osteoblasts" *J Biomed Mater Res*, Vol.47, pp.475-486, 1999.
- [7] Furukawa T, Matsusue Y, Yasunaga T, Nakagawa Y, Okada Y, Shikinami Y, Okuno M, Nakamura T, "Histomorphometric study on high-strength hydroxyapatite/poly(L-lactide) composite rods for internal fixation of bone fractures" *J Biomed Mater Res*, Vol.50, pp.410-419, 2000.
- [8] Furukawa T, Matsusue Y, Yasunaga T, Shikinami Y, Okuno M, Nakamura T, "Biodegradation behavior of ultra-high-strength hydroxyapatite/poly(L-lactide) composite rods for internal fixation of bone fractures" *Biomaterials*, Vol.21, No.9, pp.889-898, 2000.
- [9] Deng X, Hao J, Wang C, "Preparation and mechanical properties of nanocomposites of poly(D,L-lactide) with Ca-deficient hydroxyapatite nanocrystals" *Biomaterials*, Vol.22, No.21, pp.2867-2873, 2001.
- [10] Shikinami Y, Matsusue Y, Nakamura T, "The complete process of bioresorption and bone replacement using devices made of forged composites of raw hydroxyapatite particles/poly L-lactide (F-u-HA/PLLA)" *Biomaterials*, Vol.26, No.27, pp.5542-5551, 2005.
- [11] Hong Z, Zhang P, He C, Qiu X, Liu A, Chen L, Chen X, Jing X, "Nano-composite of poly (L-lactide) and surface grafted hydroxyapatite: Mechanical properties and biocompatibility" *Biomaterials*, Vol.26, No.32, pp.6296-6304, 2005.
- [12] Debra DWC, Julia AK, Darinda MM, Cho LM, "In vitro flexural properties of hydroxyapatite and self-reinforced poly(L-lactic acid)" *J Biomed Mater Res Part A*, Vol.78-A, No.3, pp.541-549, 2006.
- [13] Fang L, Yan J, Xiaodan L, Demin Jia, "Properties and Morphology of Bioceramics/Poly(D,L-lactide) Composites Modified by In situ Compatibilizing Extrusion" *J Appl Polym Sci*, Vol.102, pp.4085-4091, 2006.
- [14] Kikuchi M, Suetsugu Y, Tanaka J, "Preparation and mechanical properties of calcium phosphate/copoly-L-lactide composites" *J Mater Sci-Mater Med*, Vol.8, pp.361-364, 1997.
- [15] Verheyen CCPM, de Wijn JR, van Blitterswijk CA, de Groot K, "Evaluation of hydroxyapatite/poly(L-lactide) composites: Mechanical behavior" *J Biomed Mater Res*, Vol.26, pp.1277-1296, 1992.
- [16] Todo M, Park SD, Arakawa K, Takenoshita Y, "Relationship between microstructure and fracture behavior of bioabsorbable HA/PLLA composites." *Composites: Part A*, Vol.37, No.12, pp.2221-2225, 2006.